

New artiopodan euarthropods from the Chengjiang fauna (Cambrian, Stage 3) at Malong, Yunnan, China

YUYAN ZHU, HAN ZENG, YAO LIU, and FANGCHEN ZHAO



Zhu, Y., Zeng, H., Liu, Y., and Zhao, F. 2023. New artiopodan euarthropods from the Chengjiang fauna (Cambrian, Stage 3) at Malong, Yunnan, China. *Acta Palaeontologica Polonica* 68 (3): 427–440.

The artiopodans, consisting of trilobites and their relatives, were a major euarthropod group in the Paleozoic. Since the first discovery of *Naraoia* from the Chengjiang fauna, a significant number of artiopodans have been subsequently found in China. Here we describe three new artiopodan species from the lower Cambrian Chengjiang fauna (Cambrian Series 2, Stage 3) at Malong, Yunnan, China. *Zhugeia acuticaudata* gen. et sp. nov. is defined by a semielliptical cephalon with long genal spines, nine overlapping thoracic tergites, and a pygidium with an elongated needle-like median spine. Its cephalic shield covers multiple anterior thoracic tergites. *Tonglailia bispinosa* gen. et sp. nov. is defined by a suboval cephalon, seven thoracic tergites, and a micropygous pygidium with a pair of parallel posteriormost spines. *Sidneyia malongensis* sp. nov., a new occurrence of *Sidneyia* from South China, is defined by a crescent-shaped cephalon, eight imbricated tergites, and an abdomen consisting of two cylindrical segments and a tail fluke. The evolutionary affinities of these new taxa are reconstructed and discussed in a phylogenetic context. Phylogenetic analyses resolve *Z. acuticaudata* among the xandarellids and *T. bispinosa* gen. et sp. nov. as a trilobitomorph with an uncertain placement. The discovery of three new species improves the biodiversity of artiopodans from the Cambrian and the Chengjiang fauna.

Key words: Arthropoda, Trilobitomorpha, Vicissicaudata, Burgess Shale-type fossils, exceptional preservation, Lagerstätten, Cambrian, Yu'an-shan Formation, Chengjiang.

Yuyan Zhu [yuzhu@nigpas.ac.cn; ORCID: <https://orcid.org/0009-0005-1957-7429>], Han Zeng [hzeng@nigpas.ac.cn; ORCID: <https://orcid.org/0000-0002-5728-7896>] (corresponding author), Yao Liu [yaoliu@nigpas.ac.cn; ORCID: <https://orcid.org/0009-0007-5098-8220>], and Fangchen Zhao [fczhao@nigpas.ac.cn; ORCID: <https://orcid.org/0000-0001-8473-4439>], State Key Laboratory of Palaeobiology and Stratigraphy, Nanjing Institute of Geology and Palaeontology, Chinese Academy of Sciences, Nanjing 210008, China; University of Chinese Academy of Sciences, Beijing 100049, China.

Received 14 May 2023, accepted 18 August 2023, available online 8 September 2023.

Copyright © 2023 Y. Zhu et al. This is an open-access article distributed under the terms of the Creative Commons Attribution License (for details please see <http://creativecommons.org/licenses/by/4.0/>), which permits unrestricted use, distribution, and reproduction in any medium, provided the original author and source are credited.

Introduction

The artiopodans are major euarthropod components in the Paleozoic marine communities, notably in the Cambrian Burgess Shale-type Lagerstätten (e.g., Caron et al. 2014; Zhao et al. 2014; Fu et al. 2019). They consist of trilobites and diverse groups of trilobite-like euarthropods that feature a series of trunk appendages in similar morphology (Ortega-Hernández et al. 2013; Zhai et al. 2019). Although artiopodans have been widely regarded as crown-group euarthropods, whether artiopodans have a chelicerate or mandibulate affinity is long controversial (Scholtz and Edgecombe 2006; Budd and Telford 2009; Daley et al. 2018; Aria 2022), and it remains questionable whether artiopodans constitute a monophyletic Artiopoda Hou and Bergström, 1997, or a paraphyletic grouping (Legg et al. 2013; Aria and Caron 2017, 2019; Zeng et al. 2020). Artiopoda has been divided

into two subclades: Trilobitomorpha Størmer, 1944, and Vicissicaudata Ortega-Hernández, Legg, and Braddy, 2013. Trilobitomorpha comprises Trilobita and their non-biomineralized relatives, such as Xandarellida, Conciliterga, and Nektaspidida (Ortega-Hernández et al. 2013). Vicissicaudata comprises Aglaspidida, Cheloniellida, *Sidneyia* and related taxa (Lerosey-Aubril et al. 2017).

Since the first discovery of the nektaspidid artiopodan *Naraoia* from the Chengjiang fauna (Zhang and Hou 1985), the Chengjiang fauna has been recognized as the Cambrian Konservat-Lagerstätte with the highest generic and species diversity of non-trilobite artiopodans (e.g., Chen 2004; Caron et al. 2014; Hou et al. 2017). The recent studies on detailed appendicular morphology and ventral structures of these Chengjiang fossils have been updating the paleobiology and phylogeny of artiopodans (e.g., Zhai et al. 2019; Chen et al. 2019; Schmidt et al. 2022). To expand this re-

search area, here we describe three new artiopodans, including a xandarellid, a trilobitomorpha of uncertain affinity, and a species of *Sidneyia*, from the Chengjiang fauna at the Kuangshan section, Malong, Yunnan, China. The phylogenetic placements of these taxa are analyzed and discussed. These discoveries enrich the diversity of artiopodans from the Cambrian and the Chengjiang fauna.

Nomenclatural acts.—This published work and the nomenclatural acts it contains have been registered in ZooBank: <http://zoobank.org/urn:lsid:zoobank.org:pub:DFA660D6-B56D-4976-9442-D1185F103955>.

Institutional abbreviations.—NIGP, Nanjing Institute of Geology and Palaeontology, Chinese Academy of Sciences, China.

Geological setting

All specimens of this paper were collected from a 4 m-deep quarry of the upper part of Maotianshan Shale Member, Yu'an-shan Formation at the Kuangshan section (N 25°20'45.06", E 103°31'0.23") in Malong District, Qujing City, Yunnan Province, China, which is located at about 95 km northeastern of Chengjiang, where the Chengjiang fauna was originally discovered (Zhao et al. 2012). At Kuangshan section, the Yu'an-shan Formation is a 76 m-thick lithostratigraphic unit composed of Black Shale Member, Maotianshan Shale Member and Upper Siltstone Member in ascending order (Zhao et al. 2012). In the Malong area, the Chengjiang fossil interval of Maotianshan Shale Member comprises yellowish background mudstone intercalating with siltstone beds and minimal single-event mudstone beds, showing the mixing of background and event mudstone layers. Such mixing indicates reworking and redeposition (Zhao et al. 2012), and represents taphofacies different from the classical stacked couplets of background and event mudstone layers in the Chengjiang-Haikou area (Hu 2005). The trilobites co-occurring with the non-trilobite artiopodans described in this paper include *Wutingaspis malungensis* and *Dolerolenus (Malungia) laevigata* (Luo et al. 2008, 2015; Zhao et al. 2012), indicating that these fossils belong to the upper part of *Wutingaspis–Eoredlichia* Trilobite Zone of the undefined Cambrian Series 2, Stage 3 (Lin 2008; Zhu et al. 2019).

Material and methods

All the specimens are deposited at the Nanjing Institute of Geology and Palaeontology, Chinese Academy of Sciences (NIGP). The specimens were photographed under natural or polarized lighting by using a Nikon D810 camera with a Micro-Nikkor 105 mm f/2.8 lens, a Leica M205C stereomicroscope and a Zeiss Axio Zoom V16 stereomicroscope.

Fluorescence images were photographed under 532 nm green laser by using a Zeiss Axio Imager Z2 stereomicroscope. Greyscale images of RGB channels were extracted from the photos of fossils in Adobe Photoshop™ CS5. Interpretative drawings were made by tracing high-resolution photos in Adobe Illustrator™ CS5 and were verified by observations under stereomicroscope. Morphological terminology used in this paper mainly follows Ortega-Hernández et al. (2013).

The phylogenetic dataset in this study is composed of 69 taxa and 93 characters (see SOM, Supplementary Online Material available at http://app.pan.pl/SOM/app68-Zhu_etal_SOM.pdf). The current dataset was based on the dataset of Zhang et al. (2022) containing 65 taxa, which was updated with four taxa added, including *Sidneyia minor* Du, Bruton, Yang, and Zhang, 2023 and the three new species described herein. The character 58, length of postabdomen, was coded as two segments (state 1) for *S. minor* in Du et al. (2023), which was incorrect by referring to the morphological description of *S. minor* (Du et al. 2023). In the data matrix used in our study, this character state is revised as one segment (state 0).

The data matrix was analyzed with parsimony and Bayesian methods. The maximum parsimony analyses were conducted in TNT v.1.5 (Goloboff and Catalano 2016). All characters were treated as unordered. Each analysis, with equal or implied weighting setting of characters applied (concavity values $k = 2-10, 20, \infty$) (Goloboff 1993), consisted of a traditional search comprising 1,000 replicates of tree bisection and reconnection with 1,000 trees saved per replicate. Bootstrap, jackknife, and group present/contradicted (GC) values (Goloboff et al. 2003) were calculated for nodal supports. The results from traditional searches were verified by the New Technology searches using sectorial search, ratchet, drift, and tree fusing with finding minimum length 100 times and default settings in other searching parameters in TNT. The detailed strict consensus trees found under various concavity values can be found in the SOM: fig. 1.

The Bayesian phylogenetic inference was performed in MrBayes v.3.2.7a with default priors and Markov chain Monte Carlo (MCMC) settings (Ronquist et al. 2012). The Bayesian analysis had two runs of 50 million MCMC generations containing four chains under the Mk_v + gamma model (Lewis 2001). Trees were sampled every 1,000 generations with the first 25 percentage of samples discarded as burn-in.

Systematic palaeontology

Phylum Euarthropoda Lankester, 1904

Subphylum Artiopoda Hou and Bergström, 1997

Superclass Trilobitomorpha Størmer, 1944

Order Xandarellida Chen, Ramsköld, Edgecombe, and Zhou in Chen et al., 1996

Family uncertain

Genus *Zhugeia* nov.

ZooBank LSID: urn:lsid:zoobank.org:act:10C13356-3E01-4721-9C8E-5E30E3097946

Type species: *Zhugeia acuticaudata* gen. et sp. nov.; see below, by monotypy.

Etymology: For the Zhuge Mountain where the Kuangshan section is located and where the respected prime minister Liang Zhuge of Shu-Han once camped at about 225 A.D. during the Three Kingdoms Period of ancient China.

Diagnosis.—Semi-elliptical cephalon with a pair of genal spines. A pair of ovoid lateral eyes near anterior margin of cephalon. Cephalon posteriorly covering two thoracic tergites. Nine partially overlapping tergites with pleural spines. Micropygous pygidium with two small lateral spines and an elongated needle-like median spine.

Remarks.—The order Xandarellida is diagnosed by the semicircular cephalic shield with stalk lateral eyes which extend posteriorly to cover multiple thoracic tergites and pygidium with broad median spine (Chen et al. 1996; Ramsköld et al. 1997; Chen et al. 2019). *Zhugeia* complies with the diagnosis of Xandarellida, such as a cephalic shield covering at least two thoracic tergites and pygidium with a median spine. *Zhugeia* differs from the other xandarellids in various aspects (see more details in the Remarks of species). Thus, *Zhugeia* is a new genus of Xandarellida.

Zhugeia acuticaudata gen. et sp. nov.

Fig. 1.

ZooBank LSID: urn:lsid:zoobank.org:act:224B5712-741A-44A1-B750-1D6EDFAF5705

Etymology: From Latin *acuti* spinous and *caudata*, tail.

Holotype: NIGP 200049, specimen preserving most part of exoskeleton, part only (Fig. 1).

Type locality: Kuangshan section, Malong, Yunnan, China.

Type horizon: Maotianshan Shale Member, Yu'an-shan Formation, *Wutingspispis-Eoredlichia* Trilobite Zone, Cambrian Series 2, Stage 3.

Material.—Type material only.

Diagnosis.—As for the genus.

Description.—Suboval exoskeleton consists of cephalon, thorax, and pygidium, measuring 49 mm long (including the median spine on pygidium) and 23 mm wide.

Cephalon is semi-circular. Anterior margin of cephalon is rounded, and posterior margin is approximately straight (Fig. 1A₃; ce). A pair of broad genal spines reach posteriorly to the third thoracic tergite, measuring 19 mm long and 23 mm wide (Fig. 1A₃, D; gs). Two long ovoid lateral eyes are situated near the anterior margin of cephalon (Fig. 1A₃, B, C; e). Cephalon extends posteriorly to cover two anteriormost thoracic tergites (Fig. 1A₃, E; ct1, ct2). Cephalon excluding genal angles occupies approximately one-third of whole-body length.

Except for two anteriormost thoracic tergites covered by cephalon, thoracic region, measuring 17 mm long, consists of nine partially overlapping tergites. Tergites of thorax have overlapping areas. The average overlapping area accounts

Table 1. Measurements (in mm) of thoracic tergites of *Zhugeia acuticaudata* gen. et sp. nov., based on holotype NIGP 200049.

Thoracic tergite number	Width	Length
t4	20	1.9
t5	18	1.9
t6	17	2.2
t7	16	2.4
t8	13	2.5
t9	11	3.5

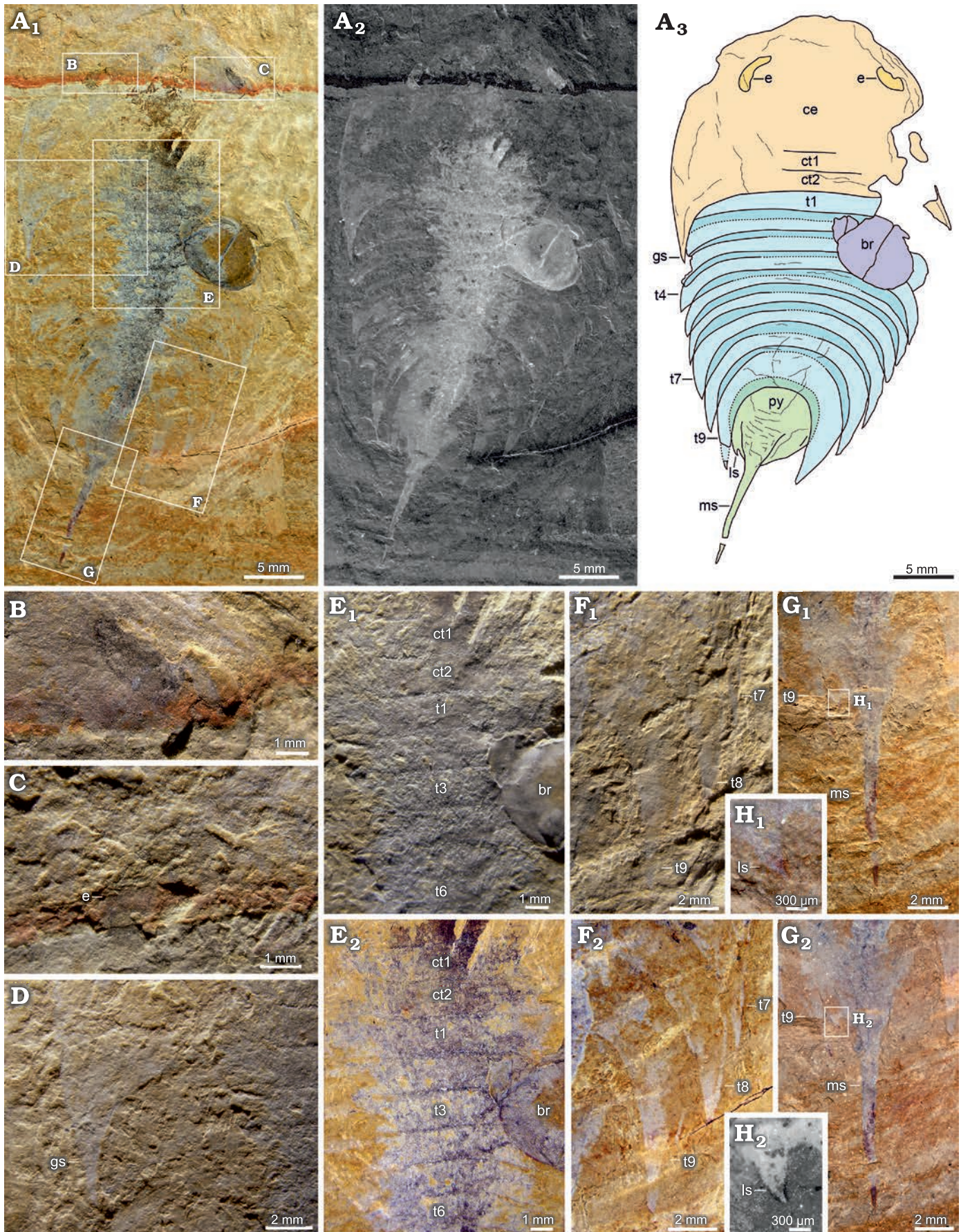
for about one-fourth to one-third of the sagittal length of the tergite. The first six thoracic tergites, which are almost equal in sagittal length, have nearly straight posterior margins (Fig. 1E: t1–t6). The last three thoracic tergites, which are progressively longer in sagittal length, are curved posteriorly (Fig. 1F: t7–t9, Table 1). Anterior thoracic tergites are almost as wide as cephalon. The fourth thoracic tergite is the broadest with maximum width of 19 mm, and following tergites narrow toward the rear. Lengths of pleural spines of thoracic tergites increase towards pygidium.

Pygidium is situated within a notch formed by pleural spines of posteriormost thoracic tergite. Teardrop-shaped pygidium, measuring 16 mm long including pygidial spine, bears a pair of triangular posterolateral pygidial spines and an elongated needle-like median pygidial spine. Median pygidial spine is slightly longer than main part of pygidial tergite (Fig. 1A₃, G; ms; Fig. 1A₃, H; ls).

Remarks.—Four genera have been erected in the order Xandarellida, including *Xandarella* Hou, Ramsköld, and Bergström, 1991, *Cindarella* Chen, Ramsköld, Edgecombe, and Zhou in Chen et al., 1996, *Luohuilinella* Zhang, Fu, and Dai, 2012, and *Sinoburius* Hou, Ramsköld, and Bergström, 1991.

The cephalon of Xandarellida shows marked morphological variations. *Zhugeia* has a pair of broad genal spines similar to *Sinoburius* (Hou and Bergström 1997; Chen et al. 2019), while *Xandarella* and *Luohuilinella* have acute genal angles rather than genal spines (Hou and Bergström 1997; Zhang et al. 2012; Hou et al. 2018), and *Cindarella* has rounded genal angles (Ramsköld et al. 1997). As in *Xandarella*, *Sinoburius*, and *Cindarella*, *Zhugeia* lacks the anterolateral eye notches typical of *Luohuilinella* (Zhang et al. 2012; Hou et al. 2018). Regarding eyes, *Zhugeia* shares anteroventral lateral eyes that are incorporated into the dorsal cephalic shield with *Xandarella* and *Sinoburius*, in contrast to a pair of lateral stalked eyes positioned at the anterolateral cephalic margin in *Luohuilinella* and *Cindarella* (Ramsköld et al. 1997; Zhang et al. 2012; Hou et al. 2018; Chen et al. 2019). *Zhugeia* has no eye slits associated with eyes that are present in *Xandarella* (Hou and Bergström 1997).

Other xandarellids exhibit different thoracic morphology from that of *Zhugeia*. The number of thoracic tergites of *Zhugeia* (9 tergites) is more than that in *Sinoburius* (7 tergites) and less than those in *Xandarella* (10 tergites), *Cindarella* (17 tergites), and *Luohuilinella* (27–30 tergites)



(Hou and Bergström 1997; Ramsköld et al. 1997; Zhang et al. 2012; Hou et al. 2018; Chen et al. 2019). As in *Xandarella*, *Luohuilinella*, and *Cindarella*, the anteriormost thoracic tergites of *Zhugeia* are almost as wide as the cephalon (Hou and Bergström 1997; Ramsköld et al. 1997; Zhang et al. 2012; Hou et al. 2018), while the anteriormost thoracic tergites of *Sinoburius* are narrower than the cephalon (Hou and Bergström 1997; Chen et al. 2019). In addition, the first thoracic tergite of *Zhugeia* is narrower than successive tergites, like *Sinoburius* (Chen et al. 2019). Thoracic tergites of *Zhugeia* narrow toward the rear, as shown in *Xandarella*, *Cindarella*, and *Luohuilinella* (Hou and Bergström 1997; Ramsköld et al. 1997; Zhang et al. 2012; Hou et al. 2018), while in *Sinoburius* first thoracic tergite is the narrowest (Hou and Bergström 1997; Chen et al. 2019).

Although all known members of Xandarellida have micropygous pygidium, their pygidia still show distinctions. Relative to width of cephalon, pygidium of *Zhugeia* is similar to that of *Xandarella* and is narrower than that of *Sinoburius* (Hou and Bergström 1997; Chen et al. 2019). *Zhugeia* has a dorsal needle-like spine like *Xandarella* instead of the broad median spine of *Sinoburius* (Hou and Bergström 1997; Chen et al. 2019). The micropygous pygidia of two species of *Luohuilinella* are smallest among xandarellids (Zhang et al. 2012; Hou et al. 2018). A terminal spine is recognized in *L. deletres* (Hou et al. 2018), but other pygidial morphologies of *Luohuilinella* are unclear (Zhang et al. 2012; Hou et al. 2018). Among xandarellids, only *Cindarella* lacks median pygidial spine (Ramsköld et al. 1997). As in *Xandarella* and *Cindarella*, *Zhugeia* has a pair of small lateral spines, while *Sinoburius* has two pairs of lateral spines (Hou and Bergström 1997; Ramsköld et al. 1997; Chen et al. 2019).

Stratigraphic and geographic range.—Type locality and horizon only.

Order and family incertae sedis

Genus *Tonglailia* nov.

ZooBank LSID: urn:lsid:zoobank.org:act:DA8A8456-AB77-4C7A-AB23-336517CD1EDE

Etymology: After *Tonglai*, an ancient name of Malong where the fossil was discovered.

Type species: *Tonglailia bispinosa* gen. et sp. nov.; see below, by monotypy.

Diagnosis.—Elliptical cephalon with a pair of marginal cephalic spines. Two oval eyes situated near the anterior margin of cephalon. Seven partially overlapping tergites with posterolateral marginal spines. Micropygous pygidium with a pair of posteriormost triangular spines.

Remarks.—The dorsal eyes of *Tonglailia* are located in an anterior position which is similar to the aglaspideid counterparts. However, the cephalon of *Tonglailia* has a rounded genal area and a unique pair of lateral marginal spines, lacking the characteristic genal spines of aglaspideids. The posterior margin of pygidium is intact, showing no evidence of the diagnostic tailspine in aglaspideids. Additionally, cuticle of *Tonglailia* is non-biomineralized, another obvious difference from aglaspideids. With these distinctions, *Tonglailia* does not comply the diagnosis of Aglaspidea and Vicissicaudata (Lerosey-Aubril et al. 2017). The presence of pygidium in *Tonglailia* is a typical character of trilobitomorph artiopodans (Ortega-Hernández et al. 2013), but *Tonglailia* is distinguished from other trilobitomorphs in several aspects, such as a suboval cephalon with special lateral marginal spines and a micropygous pygidium with two posterior spines. Therefore, *Tonglailia* represents a new genus (see details in the remarks for the type species below).

Tonglailia bispinosa gen. et sp. nov.

Fig. 2.

ZooBank LSID: urn:lsid:zoobank.org:act:259646CE-8087-4865-BA77-CEE7E47CD387

Etymology: From Latin, *bi*, double and *spinosa*, spinous.

Holotype: NIGP 200050, specimen preserving complete cephalon and most part of thorax and abdomen, part only (Fig. 2).

Type locality: Kuangshan section, Malong, Yunnan, China.

Type horizon: Maotianshan Shale Member, Yu'an-shan Formation, *Wutingaspis–Eoredlichia* Trilobite Zone, Cambrian Series 2, Stage 3.

Material.—Type material only.

Diagnosis.—As for the genus.

Description.—Oblong exoskeleton, measuring 27 mm long and 19 mm wide, is composed of cephalon, thorax, and pygidium.

Cephalon is subelliptic to subrectangular, measuring 11 mm long and 16 mm wide (Fig. 2A₃: ce). Anterior margin of cephalon is rounded, and posterior margin is approximately straight. Cephalon has a pair of triangular marginal spines located almost halfway on cephalic lateral margin (Fig. 2A₃, C, D: cs). Two rimmed oval eyes are located close to anterior cephalic margin (Fig. 2B: e). A pair of flap-like structures, presumably appendages, are present beyond cephalon lateral margins (Fig. 2E: ap?). Some marginal lines can be found around cephalon (Fig. 2C, D: ml). The numerous wrinkles near the anterior and lateral cephalic margins indicate convexity of cephalon.

Thorax consists of seven partially overlapping tergites with subequal sagittal lengths, measuring 15 mm long. For

← Fig. 1. Artiopodan euarthropod *Zhugeia acuticaudata* gen. et sp. nov. from the Cambrian Stage 3 Chengjiang fauna at Malong, Yunnan, China; holotype NIGP 200049. **A.** Whole specimen, under high-angle light (A₁), inverted red channel image (A₂), interpretative drawing (A₃). **B.** Right eye. **C.** Left eye. **D.** Left genal spine. **E.** Thoracic tergites under low-angle light (E₁), under high-angle light (E₂). **F.** Sixth to ninth thoracic tergites under low-angle light (F₁), under high-angle light (F₂). **G.** Median pygidial spine under low-angle light (G₁), under high-angle light (G₂). **H.** Lateral pygidial spine under low-angle light (H₁), fluorescence photograph under 532 nm green laser (H₂). Abbreviations: br, bradoriid; ce, cephalon; ct1–ct2, thoracic tergite number covered by cephalon; e, eye; gs, genal spine; ls, lateral pygidial spine; ms, median pygidial spine; py, pygidium; t1–t9, thoracic tergites.

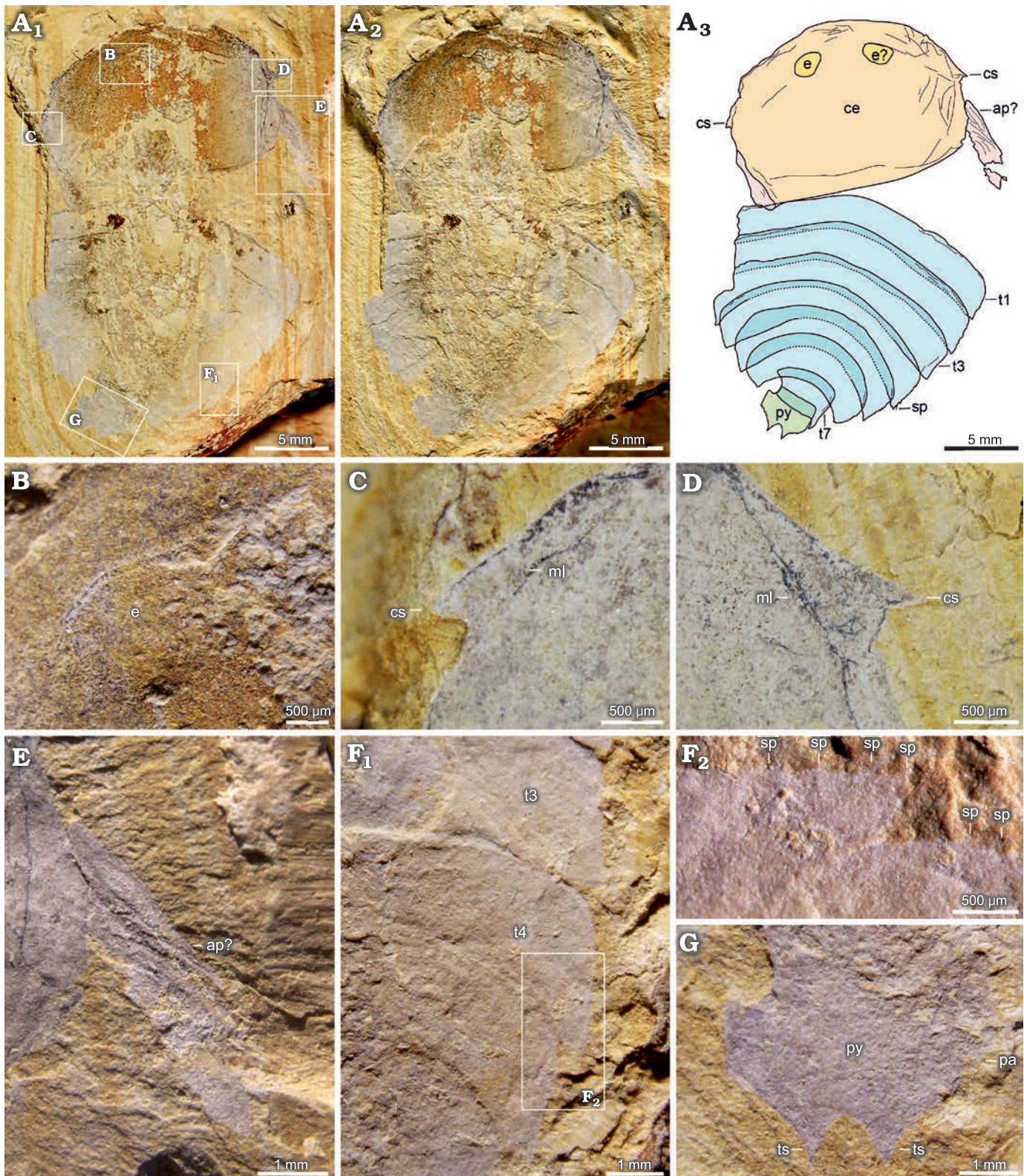


Fig. 2. Artiopodan euarthropod *Tonglailia bispinosa* gen. et sp. nov. from the Cambrian Stage 3 Chengjiang fauna at Malong, Yunnan, China; holotype NIGP 200050. A. Whole specimen under high-angle light (A₁), under low-angle light (A₂), interpretative drawing (A₃). B. Left eye. C. Left cephalic spine. D. Right cephalic spine. E. Right appendage. F. Thoracic tergites (F₁) with spines (F₂). G. Pygidium. Abbreviations: ap, appendage; ce, cephalon; cs, cephalic spine; e, eye; ml, marginal line around cephalon; pa, pleural angle; py, pygidium; sp, marginal spine; t1–t7, thoracic tergites; ts, terminal spine.

the first to fourth thoracic tergites, overlapping area between adjacent tergites accounts for about one-fifth of the

sagittal length of tergite. Overlapping area among last three thoracic tergites is approximately one-third of the sagit-

Table 2. Measurements (in mm) of thoracic tergites of *Tonglailia bispinosa* gen. et sp. nov., based on holotype NIGP 200050.

Thoracic tergite number	Width	Length
t1	19	2.0
t2	18	2.3
t3	16	2.3
t4	14	2.5
t5	11	2.8
t6	8	3.2
t7	4	2.7

tal length of the tergite. Thoracic tergites gradually curve backwards. Widths of first two tergites are close, approximately 19 mm wide (Fig. 2A₃; t1–t3; Table 2), and widths of more posterior thoracic tergites are narrowing towards rear (Table 2). Pleural angles of the first six thoracic tergites exhibit a similar shape absent elongate spine. Pleural angle of the last thoracic tergite forms a spine towards the pygidium (Fig. 2G: pa). Pleural angles of thoracic tergites have numerous tiny marginal spines (Fig. 2F: sp).

Pygidium is micropygous and subrectangular in shape measuring 3 mm long and 4 mm wide (Fig. 2A₃; py; G: py, ts). Width of pygidium is slightly narrower than that of posteriormost thoracic tergite. Posterior pygidial margin bears a pair of closely spaced robust triangular spines that form a notch between pygidial spines, measuring approximately 1 mm wide. Margin of notch is smooth and featureless.

Remarks.—The cephalic spines present in most of non-trilobite arthropods are located at the genal angles (Hou and Bergström 1997), but *Tonglailia* has its cephalic marginal spines placed halfway on the cephalon. The teardrop-shaped lateral eyes that form bulges on the anterior cephalic shield are analogous to the helmetiid counterparts, such as *Helmetia*, *Kuamaia*, and *Saperion*, but *Tonglailia* bears no anterior sclerite associated with eyes in helmetiids (Hou and Bergström 1997; Edgecombe and Ramsköld 1999). Among trilobitomorpha, the extensive overlapping of thoracic tergites in *Tonglailia* is most comparable to that of xandarellids (Hou and Bergström 1997). The micropygous pygidium is found in most xandarellids and some other trilobitomorpha like *Zhiwenia* and *Longquania*, and the pygidium with a pair of posteriormost spines is shared by *Tonglailia* and *Longquania* (Luo et al. 2008; Hu et al. 2013; Du et al. 2018). The difference is that the notch formed by the pygidial spines in *Tonglailia* is smooth, but the notch in *Longquania* bears serrated spines (Luo et al. 2008; Hu et al. 2013). In addition, phylogenetic analyses suggest that the evolutionary affinity of *Tonglailia* is uncertain (see below).

Stratigraphic and geographic range.—Type locality and horizon only.

Superclass Vicissicaudata Ortega-Hernández, Legg, and Braddy, 2013

Order and family incertae sedis

Genus *Sidneyia* Walcott, 1911

Type species: *Sidneyia inexpectans* Walcott, 1911, Walcott Quarry, Fossil Ridge, British Columbia, Canada; the Phyllopod Bed, Burgess Shale Formation.

Emended diagnosis.—Cephalon consisting of a rectangular dorsal shield with large hypostome, lateral cephalic notches for accommodation of stalked eyes and antennae, and three pairs of isomorphic post-antennal appendages. Thorax of eight to ten articulating tergites, each of which bears a pair of biramous limbs. Abdomen of one to three cylindrical sclerites and a telson with a pair of tail flukes (emended from Du et al. 2023).

Remarks.—With the recent discovery of *S. minor* from the lower Cambrian Hongjingshao Formation of Yunnan, China (Du et al. 2023), the diagnosis of the originally monospecific *Sidneyia* was updated to accommodate the morphology of *S. minor*. As the new species established here is resolved as a sister species to the two other species of *Sidneyia* (see below), the diagnosis of *Sidneyia* is emended by incorporating the morphology of this new species, which includes different numbers of thoracic tergites and abdominal segments.

Sidneyia malongensis sp. nov.

Figs. 3, 4.

ZooBank LSID: urn:lsid:zoobank.org:act:4BDF80F-1323-4748-BBB6-4A5846D9ED00

Etymology: After Malong District where the fossil was discovered.

Type material: Holotype, specimen preserving complete abdomen and most part of cephalon and thorax, part only, NIGP 200051 (Fig. 3). Paratype, specimen preserving complete abdomen, most part of thorax, and a small part of cephalon only, part only, NIGP 200052 (Fig. 4).

Type locality: Kuangshan section, Malong, Yunnan, China.

Type horizon: Maotianshan Shale Member, Yu'an-shan Formation, *Wutingspis–Eoredlichia* Trilobite Zone, Cambrian Series 2, Stage 3.

Material.—Type material only.

Diagnosis.—A species of *Sidneyia* with eight imbricated tergites in thorax and two cylindrical segments in abdomen.

Description.—Oval-shaped exoskeleton is composed of cephalon, thorax, and abdomen. Body length is about 31 mm in the holotype, and the maximum width is about 21 mm in the holotype and 15 mm in the paratype.

Cephalon is semi-elliptical, measuring 6 mm long and 17 mm wide in holotype (Fig. 3A₃: ce). Anterior margin of cephalon is rounded, and posterior margin of cephalon is straight. Lateral eyes are located at genal angles of cephalon (Fig. 3B: e). Eyes are associated with notches on cephalon, but eye stalks are unclear (Fig. 3B: n). Presence of numerous wrinkles near the anterior margin indicates the convexity of the cephalon.

Thorax consists of eight imbricated tergites of approximately equal length, measuring 16 mm long in holotype and 12 mm long in paratype. Overlapping area between adjacent thoracic tergites accounts for about one third of sagittal length of tergite. Posterior margin of the first to three thoracic tergites is almost straight. Thorax is widest at

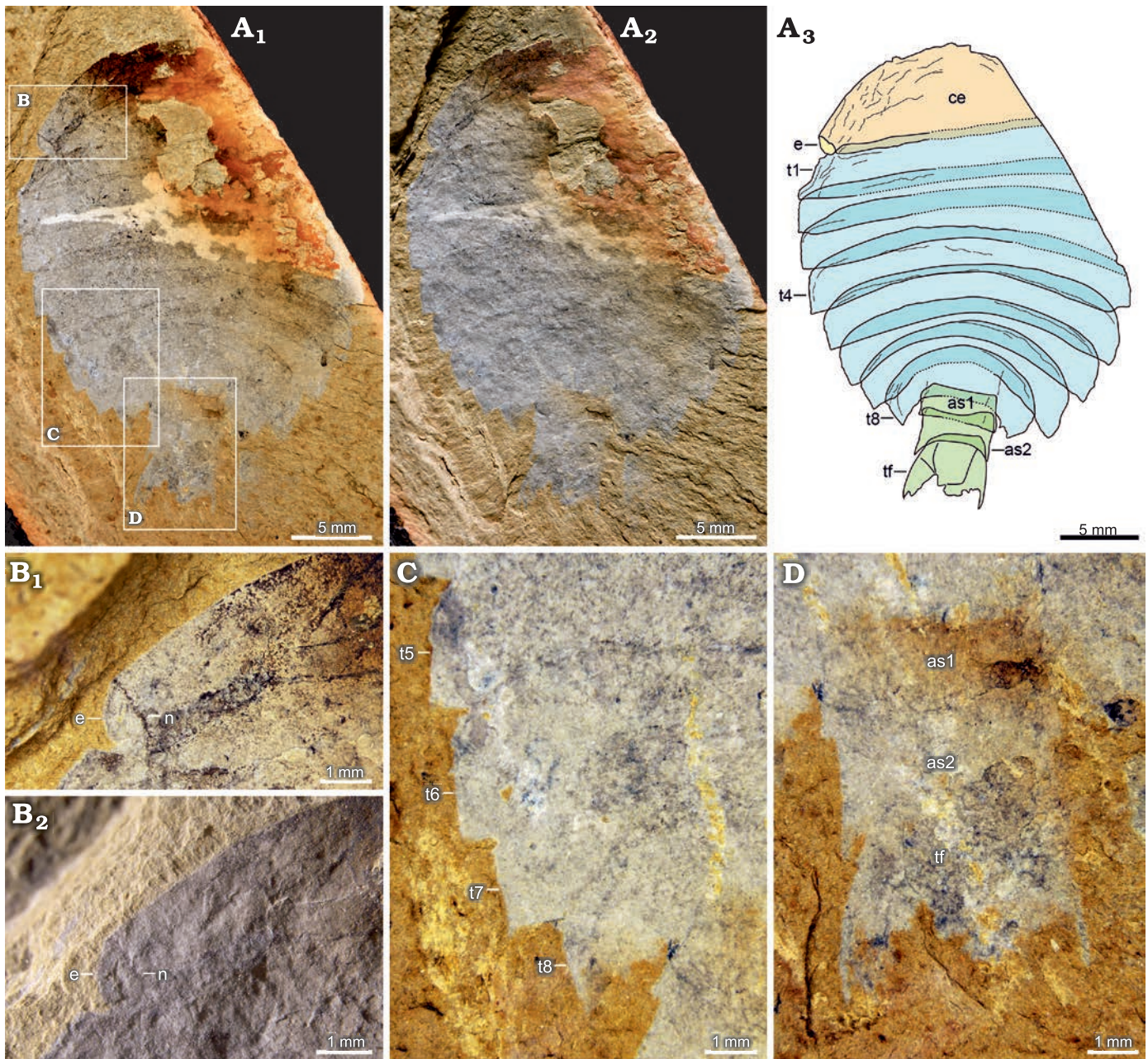


Fig. 3. Artiopodan euarthropod *Sidneyia malongensis* sp. nov. from the Cambrian Stage 3 Chengjiang fauna at Malong, Yunnan, China; holotype NIGP 200051. **A.** Whole specimen under high-angle light (**A₁**), under low-angle light (**A₂**), interpretative drawing (**A₃**). **B.** Left eye under high-angle light (**B₁**), under low-angle light (**B₂**). **C.** Fourth to eighth thoracic tergites. **D.** Abdomen. Abbreviations: as1–as2, abdominal segments; ce, cephalon; e, eye; t1–t8, thoracic tergites; tf, tail fluke.

the third or fourth thoracic tergite, measuring 8 mm wide in holotype, after which it gradually narrows and curves posteriorly (Figs. 3A₃, 4A₃; t1–t8). Pleural angle of each tergite is nearly equal along thorax. No marginal spines are found on thoracic tergites.

Abdomen consists of two overlapping cylindrical segments of subequal dimensions, measuring 4 mm long and 4 mm wide in holotype, and a tail fluke (Figs. 3A₃, D, 4A₃, C: as, tf). Abdominal segments are narrower than the last thoracic tergite. Overlapping area between adjacent abdominal segments accounts for about one-fifth to one-fourth of

sagittal length of segment, with an average length of 1 mm. Tail fluke consists of a central triangular telson and a pair of flanked flaps, which is approximately as long as abdominal segments (Figs. 3A₃, D, 4A₃, C: tf).

Remarks.—*Sidneyia malongensis* sp. nov. shares some common features with *S. inexpectans* from the Burgess Shale and *S. minor* from the Hongjingshao Formation, such as a semi-circular cephalon, a similar overlapping degree of tergites and a cylindrical abdomen (Bruton 1981; Stein 2013; Zacaï et al. 2016; Du et al. 2023). However, there are detailed morphological differences between *S. malongensis* sp. nov. and

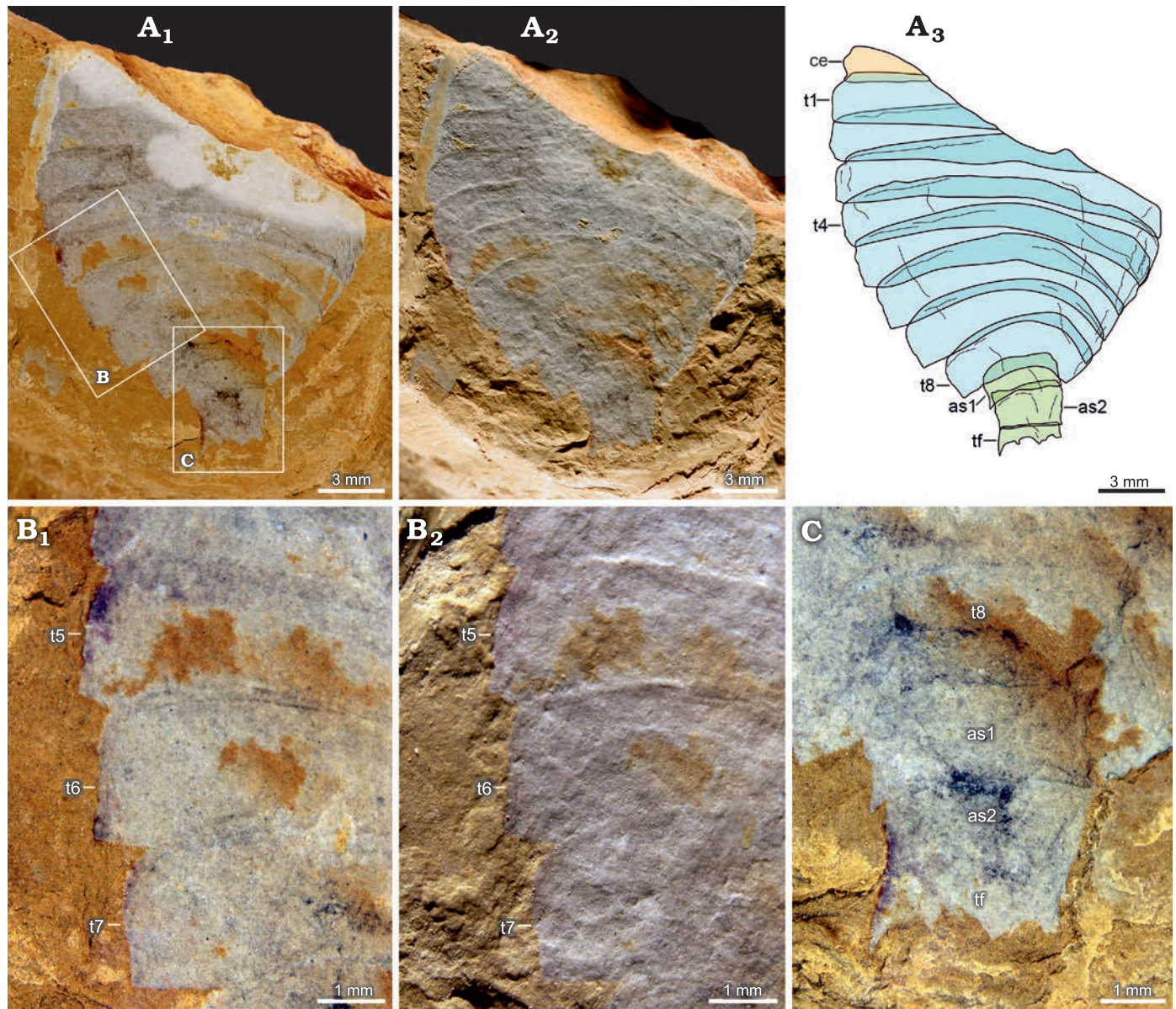


Fig. 4. Artipodan euarthropod *Sidneyia malongensis* sp. nov. from the Cambrian Stage 3 Chengjiang fauna at Malong, Yunnan, China; paratype NIGP 200052. A. Whole specimen under high-angle light (A₁), under low-angle light (A₂), interpretative drawing (A₃). B. Thoracic tergites under high-angle light (B₁), under low-angle light (B₂). C. Abdomen. Abbreviations: as1–as2, abdominal segments; ce, cephalon; e, eye; t1–t8, thoracic tergites; tf, tail fluke.

Table 3. Comparative measurements (in mm) of *Sidneyia inexpectans* Walcott, 1911, *Sidneyia cf. inexpectans* Walcott, 1911, *Sidneyia minor* Du, Bruton, Yang, and Zhang, 2023, and *Sidneyia malongensis* sp. nov. Abbreviations: al, abdomen length (telson excluded); aw, abdomen width (telson excluded); bl, body length; bw, body width; cl, cephalon length; cw, cephalon width; na, number of abdominal segments; nt, number of thoracic tergites. Note that the number of abdominal segments in *S. inexpectans* has been interpreted as two or three by different studies.

Species	Specimen number	bl	bw	cl	cw	al	aw	cl/cw	al/aw	nt	na	Reference
<i>Sidneyia inexpectans</i>	USNM139676	94	54	13	36	22	16	0.36	1.38	9	3	Stein 2013
	USNM 269165	85	46	13	34	20	16	0.38	1.25	9	2	Zacai et al. 2016
	ROM 63377	98	59	11	44	26	21	0.25	1.24	9	2	Zacai et al. 2016
<i>Sidneyia cf. inexpectans</i>	NIGP 170198	83	51	12	35	18	15	0.34	1.20	9	3	Sun et al. 2020
<i>Sidneyia minor</i>	YKLP 12435	23	14	4	13	2	3	0.31	0.67	10	1	Du et al. 2023
<i>Sidneyia malongensis</i> sp. nov.	NIGP 200051	31	21	6	17	4	4	0.35	1.00	8	2	this study

the other two species of *Sidneyia*. Comparing to the other two species of *Sidneyia*, *S. malongensis* sp. nov. has fewer thoracic tergites. *Sidneyia malongensis* sp. nov. and *S. inexpectans*

share approximately equal pleural angles along the body, but the pleural angles of *S. minor* become more acute after the seventh thoracic tergite (Bruton 1981; Stein 2013;

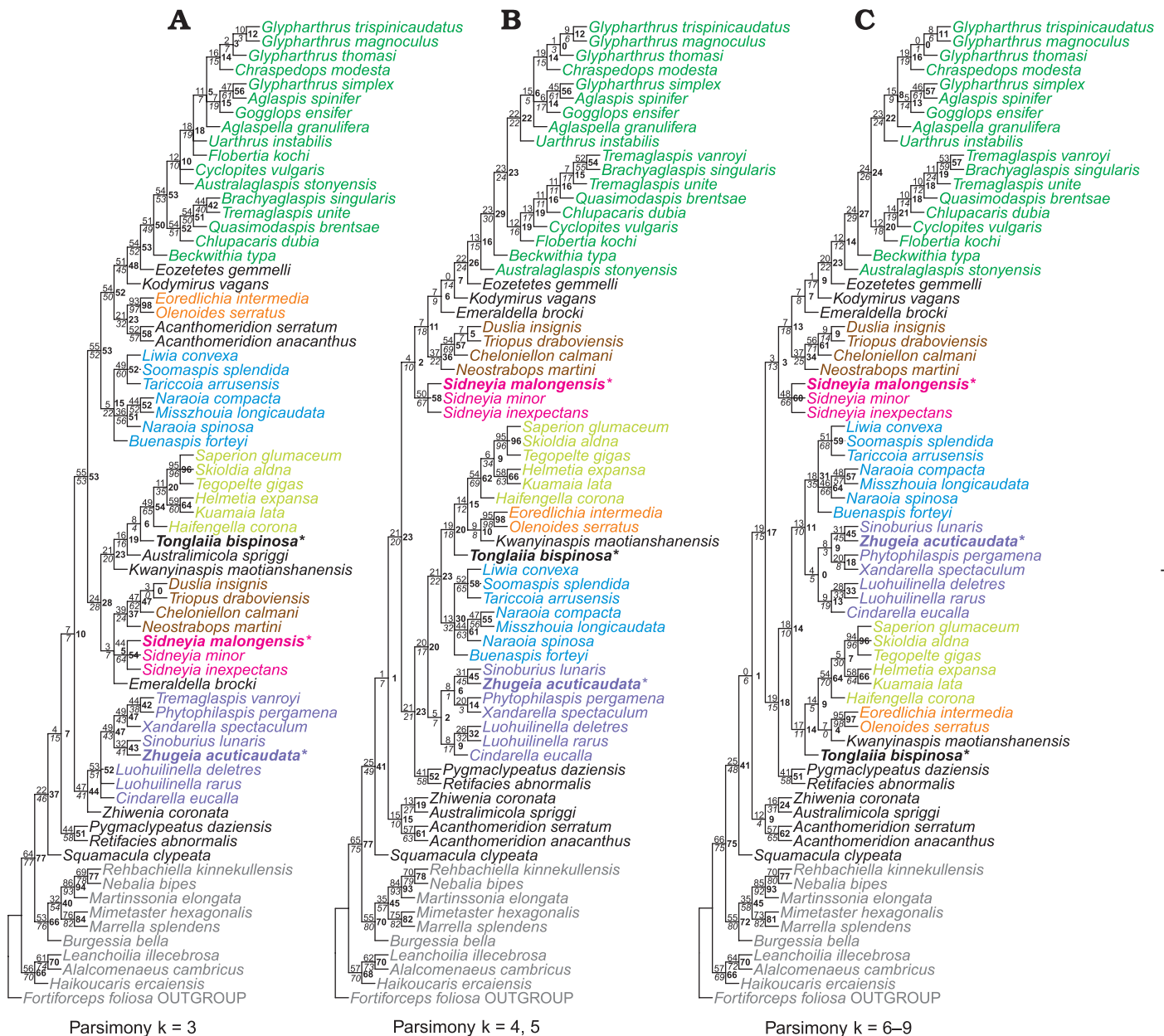
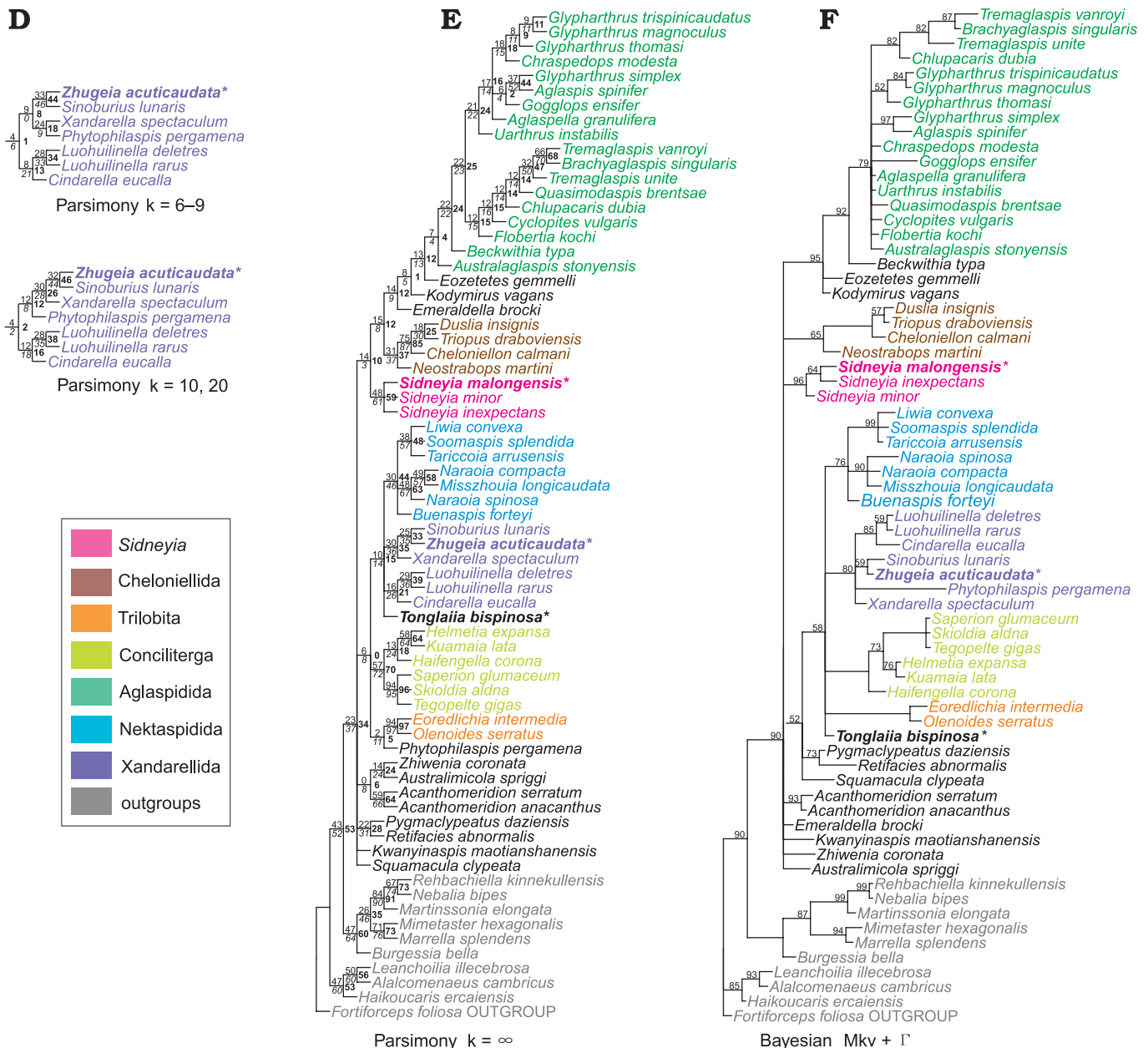


Fig. 5. Phylogenetic reconstruction of Artipoda showing the placements of *Zhugeia acuticaudata*, *Tonglailia bispinosa* gen. et sp. nov., and *Sidneyia malongensis* sp. nov. The three new artiopodan species are in bold and asterisked. A–E. Strict consensus trees from parsimony analyses. Bootstrap, jackknife and group present/contradicted supports are placed at the top left, bottom left, and middle right of nodes and are in regular, italics and bold, respectively. Nodal supports are all in percentage, and those of 100 are not shown. Individual trees can be found in the SOM: fig. 1A–D. Results from using implied weighting of characters under various concavity values k . A. $k = 3$. Note that the result with $k = 2$ differs from that with $k = 3$ only in the placement of *Neostrabops martini* and the relationships between cheloniellids. B. $k = 4, 5$. C. $k = 6–9$. D. Results under $k = 10, 20$ only differ from those under $k = 6–9$ in the interrelationships of Xandarellida. E. Results from using equal weighting of characters, where concavity value $k = \infty$. F. 50% majority-rule consensus tree from Bayesian inference under the Mkv + gamma model. Nodal supports represent posterior probabilities in percentage, and those of 100 are not shown.

Zacai et al. 2015; Du et al. 2023). The numbers of abdominal segments vary among *Sidneyia* species. The abdomen of *S. malongensis* sp. nov. has two cylindrical segments, the abdomen of *S. inexpectans* consists of three segments, and that of *S. minor* only bears one segment (Bruton 1981; Du et al. 2023). The morphology of tail fluke in *S. malongensis* sp. nov. is more similar to that of *S. inexpectans*, which has a central telson of similar length to the flanked flaps (Bruton 1981). By comparison, the tail fluke of *S. minor* has a notch

between the two flanked flaps formed by the shorter central telson (Du et al. 2023).

The four species of *Sidneyia* show differences in size and numbers of thoracic tergites and abdominal segments (Table 3). The body sizes of the lower Cambrian Series 2 *S. malongensis* sp. nov. and *S. minor* are smaller than that of the middle Cambrian Miaolingian *S. inexpectans* and *S. cf. inexpectans*. *Sidneyia malongensis* sp. nov. has the least thoracic tergites among the genus. It also has two abdominal



segments, *Sidneyia minor* has one, while *S. inexpectans* has two or three. The remarkable difference in abdominal length-width ratio also distinguishes these species. The abdominal length-width ratio of *S. malongensis* sp. nov. is roughly 1, those of *S. inexpectans* and *S. cf. inexpectans* are significantly larger (1.20–1.38), while that of *S. minor* is smaller (0.67).

Stratigraphic and geographic range.—Type locality and horizon only.

Discussion

Phylogenetic analysis.—Comparing to previous results, the resultant phylogenetic trees under the same analytical settings exhibit broad similarities in topology (Ortega-Hernández et

al. 2013; Lerosey-Aubril et al. 2017; Du et al. 2018). In our analysis, differences among the trees under various concavity constants *k* primarily manifest the changing internal relationship within Trilobitomorpha. The unstable topologies under different concavity values *k* are likely caused by character homoplasy, as such uncertainty in topology has been present since the original version of this data matrix (Ortega-Hernández et al. 2013). The available characters in the current dataset are unable to effectively resolve the exact interrelationship between the trilobitomorph groups.

Under parsimony analyses and Bayesian inference, the phylogenetic analysis consistently resolved *Zhugeia acuticaudata* as a member of Xandarellida (Fig. 5). This is supported by the synapomorphies of Xandarellida with the presences of the cephalon covering multiple anterior terg-

ites and the articulation of cephalon with reduced thoracic tergite (characters 47 and 48). In all analyses, *Zhugeia* is retrieved as a sister taxon to *Sinoburius* by the presence of acute genal spine (character 36). However, the interrelationships within Xandarellida exhibit uncertainties in the analyses. With *Zhugeia* added to the phylogenetic analyses, the resultant trees show some new topologies compared to the previous studies concerning Xandarellida (e.g., Chen et al. 2019). In most conditions of parsimony and Bayesian analyses, *Cindarella* is the sister taxon to the two species of *Luohuilinella*, which is supported by the presence of cephalon with lateral notches (character 89) (Fig. 5B–F). Only under concavity values $k = 2$ and 3 , *Cindarella* and *Luohuilinella* form an unresolved polytomy with other xandarellids (Fig. 5A; SOM: fig. 1A, B). By comparison, earlier studies only resolve a monophyletic group composed of *Cindarella* and *Luohuilinella* with $k = 4$ (Chen et al. 2019). The sister taxon of the clade consisting of *Zhugeia* and *Sinoburius* is *Xandarella* under parsimony analysis using concavity values $k = 10, 20$ and ∞ . This sister taxon depends on the presence of pygidium with lateral spines (character 66) and the absence of median spine (character 65) (Fig. 5D, E). The *Zhugeia* + *Sinoburius* clade is the sister taxon to *Xandarella* + *Phytophilaspis* with $k = 4–9$ (Fig. 5B–D) and *Xandarella* + (*Phytophilaspis* + *Tremaglaspsis vanroyi*) with $k = 2$ and 3 (Fig. 5A; SOM: fig. 1A, B). Such a close relationship between *Xandarella* and *Phytophilaspis* is supported by their shared eye slit (character 23) (Fig. 5A–C; Chen et al. 2019). Under Bayesian inference, *Phytophilaspis* also shows an affinity with xandarellid (Fig. 5F). However, *Phytophilaspis* is allied with the trilobites in the parsimony analysis under equal weighting (Fig. 5E). The inclusion of the aglaspid *T. vanroyi* within Xandarellida is based on the presence of articulation with reduced tergites (character 48), which is a common feature of Xandarellida that is only found outside xandarellids in *T. vanroyi* (Fig. 5A). However, under the parsimony analyses with concavity values $k = 4–10, 20, \infty$, and the Bayesian inference (Fig. 5B–F), *Tremaglaspsis vanroyi* is the sister taxon to *Brachyaglaspsis* in Aglaspidida by the presence of the medial cleft of tail-spine (character 71).

Tonglailia bispinosa gen. et sp. nov. is resolved within Trilobitomorpha under all analyses on the basis of the presence of pygidium (character 62), but the parsimony analysis with equal character weighting and the Bayesian inference are unable to resolve the exact position of *Tonglailia* among Trilobitomorpha (Fig. 5E, F). Under concavity values $k = 2$ and 3 (Fig. 5A; SOM: fig. 1A, B), *Tonglailia* is recovered as the sister taxon to Conciliterga, possibly based on the presence of dorsal exoskeletal bulge (character 22). However, *Tonglailia* differs from Conciliterga in several important morphological aspects. For example, *Tonglailia* has extensive overlapping of tergites, while members of Conciliterga commonly exhibit edge-to-edge pleural articulations (character 44). Under concavity values $k = 2$ and 3 , *Tonglailia* also exhibits a close affinity with *Australimicola* (Fig. 5A;

SOM: fig. 1A, B), which is supported by unclear synapomorphies. The placement of *Australimicola* itself is unstable, such that *Australimicola* is the sister taxon to *Zhiwenia* under equal weighting and $k = 4–20$ (Fig. 5B–D), presumably as the result of the presence of reflexed trunk tergites and marginal spines on tailspine in both taxa (characters 50 and 70). Under concavity values $k = 4–20$, a sister-group relationship is retrieved between *Tonglailia* and the clade Conciliterga + (Trilobita + *Kwanyinaspis*) (Fig. 5B–D). The character supporting this grouping is the dorsal exoskeletal bulge (character 22), while the latter clade is supported by the edge-to-edge pleural articulation of tergites (character 44). However, it should be noted that at concavity values $k = 2$ and 3 (Fig. 5A; SOM: fig. 1A, B), Trilobita is retrieved as the sister group of *Acanthomeridion*, as supported by their shared ecdysial sutures (characters 31 and 32). Such a result has been interpreted as an artifact in earlier studies (Ortega-Hernández et al. 2013).

In all the phylogenetic analyses, *S. malongensis* sp. nov. consistently falls within the genus *Sidneyia* (Fig. 5), which is based on the presence of tail fluke or paddle-shaped tail-spine (character 68) and head shield with lateral notches (character 89). The parsimony analyses recover the three species of *Sidneyia*, *S. inexpectans*, *S. malongensis* sp. nov., and *S. minor*, in a polytomy (Fig. 5A–E). The Bayesian inference, however, retrieves *S. inexpectans* and *S. malongensis* sp. nov. as sister species and *S. minor* as the earliest branching species in *Sidneyia* (Fig. 5F). The key difference between the character states of the three species of *Sidneyia* is the number of segments of postabdomen (character 58). However, *S. inexpectans*, *S. malongensis* sp. nov. and *S. minor* all have different numbers of postabdominal segments, making the synapomorphies of the sister grouping of *S. inexpectans* and *S. malongensis* sp. nov. unclear. Therefore, the interspecific relationships within *Sidneyia* resolved by the Bayesian inference remain questionable (Fig. 5F).

Palaeogeography.—*Sidneyia*, originally was an iconic euarthropod from the Burgess Shale, now includes four identified species. The type species *S. inexpectans* occurred in Laurentia (Cambrian Miaolingian, Wuliuan; British Columbia, Canada) (Bruton 1981). *S. cf. inexpectans* has been found in North China (Wuliuan; Shandong, China) (Sun et al. 2020). *S. minor* and *S. malongensis* are distributed in South China (Cambrian Stage 3; Yunnan, China) (Du et al. 2023). The known geographic distribution of *Sidneyia* shows a cosmopolitan pattern. The early Cambrian species of *Sidneyia* from South China are smaller than the middle Cambrian *Sidneyia* from Laurentia and North China (Table 3). Autecological studies interpret *Sidneyia* as an epifaunal vagrant hunter or scavenger (Caron and Jackson 2008). As adult individuals of *Sidneyia* can reach 160 mm (Bruton 1981) and it shall have limited migration capability, a plausible explanation of their cosmopolitan distribution is that their larvae or juveniles may have the potential to disperse by drifting with ocean currents.

Conclusions

The three new artiopodan euarthropods from the Cambrian Chengjiang fauna at Kuangshang section, Malong show that *Zhugeia acuticaudata* is a new xandarellid that is the sister species to *Sinoburius lunaris*, that *Tonglaia bispinosa* gen. et sp. nov. is closely related to *Conciliterga*, and that *Sidneyia malongensis* sp. nov. is a new species of *Sidneyia* from South China. These artiopodan species from the Malong area have not been found in the other fossil localities of the Chengjiang fauna, providing new insights into the differentiated spatial distribution of the Chengjiang fauna across eastern Yunnan and enrich the diversity of non-trilobite artiopodans from the Cambrian. The discovery of the oldest known species of *Sidneyia* from the Chengjiang fauna suggests a link to the Burgess Shale-type faunas of North America and strengthens a possible Cambrian biogeographic connection between South China and Laurentia.

Acknowledgements

We are grateful to Professor Shixue Hu (Chengdu Center, China Geological Survey, Chengdu, China) in the field excursions of the fossil collection. We sincerely thank Javier Ortega-Hernández (Harvard University, Cambridge, USA) and Russell Bicknell (University of New England, Armidale, Australia) for their useful comments on our manuscript. This study was supported by the National Key Research and Development Program of China (2021YFA0718100, 2022YFF0800100), the National Natural Science Foundation of China (42272019, 42072006), and the Youth Innovation Promotion Association of Chinese Academy of Sciences (2023322).

References

- Aria, C. 2022. The origin and early evolution of arthropods. *Biological Reviews* 97: 1786–1809.
- Aria, C. and Caron, J.-B. 2017. Burgess Shale fossils illustrate the origin of the mandibulate body plan. *Nature* 545: 89–92.
- Aria, C. and Caron, J.-B. 2019. A middle Cambrian arthropod with chelicerae and proto-book gills. *Nature* 573: 586–589.
- Bruton, D.L. 1981. The arthropod *Sidneyia inexpectans*, Middle Cambrian, Burgess Shale, British Columbia. *Philosophical Transactions of the Royal Society B: Biological Sciences* 295: 619–653.
- Budd, G.E. and Telford, M.J. 2009. The origin and evolution of arthropods. *Nature* 457: 812–817.
- Caron, J.-B. and Jackson, D.A. 2008. Paleoeecology of the greater phyllopod bed community, Burgess Shale. *Palaeogeography, Palaeoclimatology, Palaeoecology* 258: 222–256.
- Caron, J.-B., Gaines, R.R., Aria, C., Mángano, M.G., and Streng, M. 2014. A new phyllopod bed-like assemblage from the Burgess Shale of the Canadian Rockies. *Nature Communications* 5: 3210.
- Chen, J.Y., Zhou, G.Q., Zhu, M.Y., and Ye, G.Y. 1996. *The Chengjiang Biota: A Unique Window of the Cambrian Explosion* [in Chinese]. 222 pp. Museum of Natural Science, Taizhong.
- Chen, J.Y. 2004. *The Dawn of Animal World* [in Chinese]. 366 pp. Jiangsu Science and Technology Publishing House, Nanjing.
- Chen, X.H., Ortega-Hernández, J., Wolfe, J.M., Zhai, D.Y., Hou, X.G., Chen, A., Mai, H.J., and Liu, Y. 2019. The appendicular morphology of *Sinoburius lunaris* and the evolution of the artiopodan clade Xandarellida (Euarthropoda, early Cambrian) from South China. *BMC Evolutionary Biology* 19: 1–20.
- Daley, A.C., Antcliffe, J.B., Drage, H.B., and Pates, S. 2018. Early fossil record of Euarthropoda and the Cambrian Explosion. *Proceedings of the National Academy of Sciences of the United States of America* 115: 5323–5331.
- Du, K.S., Ortega-Hernández, J., Yang, J., and Zhang, X.G. 2018. A soft-bodied euarthropod from the early Cambrian Xiaoshiba Lagerstätte of China supports a new clade of basal artiopodans with dorsal ecdysial sutures. *Cladistics* 35: 269–281.
- Du, K.S., Bruton, D., Yang, J., and Zhang, X.G. 2023. An early Cambrian *Sidneyia* (Arthropoda) resolves the century-long debate of its head organization. *Science China Earth Sciences* 66: 521–527.
- Edgecombe, G.D. and Ramsköld, L. 1999. Relationships of Cambrian Arachnata and the systematic position of Trilobita. *Journal of Paleontology* 73: 263–287.
- Fu, D.J., Tong, G.H., Dai, T., Liu, W., Yang, Y.N., Zhang, Y., Cui, L.H., Li, L.Y., Yun, H., Wu, Y., Sun, A., Liu, C., Pei, W.R., Gaines, R.R., and Zhang, X.L. 2019. The Qingjiang biota—a Burgess Shale-type fossil Lagerstätte from the early Cambrian of South China. *Science* 363: 1338–1342.
- Goloboff, P.A. 1993. Estimating character weights during tree search. *Cladistics* 9: 83–91.
- Goloboff, P.A. and Catalano, S.A. 2016. TNT version 1.5, including a full implementation of phylogenetic morphometrics. *Cladistics* 32: 221–238.
- Goloboff, P.A., Farris, J.S., Källersjö, M., Oxelman, B., Ramírez, M.J., and Szumik, C.A. 2003. Improvements to resampling measures of group support. *Cladistics* 19: 324–332.
- Hou, X.G. and Bergström, J. 1997. Arthropods of the lower Cambrian Chengjiang fauna, southwest China. *Fossils and Strata* 45: 1–116.
- Hou, X.G., Ramsköld, L., and Bergström, J. 1991. Composition and preservation of the Chengjiang fauna—a Lower Cambrian soft-bodied biota. *Zoologica Scripta* 20: 395–411.
- Hou, X.G., Siveter, D.J., Siveter, D.J., Aldridge, R.J., Cong, P.Y., Gabbott, S.E., Ma, X.Y., Purnell, M.A., and Williams, M. 2017. *The Cambrian Fossils of Chengjiang, China: The Flowering of Early Animal Life*. 328 pp. John Wiley & Sons, Kunming.
- Hou, X.G., Williams, M., Sansom, R., Siveter, D.J., Siveter, D.J., Gabbott, S., Harvey, T.H., Cong, P.Y., and Liu, Y. 2018. A new xandarellid euarthropod from the Cambrian Chengjiang biota, Yunnan Province, China. *Geological Magazine* 156: 1375–1384.
- Hu, S.X. 2005. Taphonomy and palaeoecology of the Early Cambrian Chengjiang biota from eastern Yunnan, China. *Berliner Paläobiologische Abhandlungen* 7: 182–185.
- Hu, S.X., Zhu, M.Y., Luo, H.L., Steiner, M., Zhao, F.C., Li, G.X., Liu, Q., and Zhang, Z.F. 2013. *The Guanshan Biota* [in Chinese, with English summary]. 204 pp. Yunnan Science and Technology Press, Kunming.
- Lankester, E.R. 1904. The structure and classification of Arthropoda. *Quarterly Journal of Microscopical Science* 47: 525–582.
- Legg, D.A., Sutton, M.D., and Edgecombe, G.D. 2013. Arthropod fossil data increase congruence of morphological and molecular phylogenies. *Nature Communications* 4: 2485.
- Lerosey-Aubril, R., Zhu, X.J., and Ortega-Hernández, J. 2017. The Vicissicaudata revisited—insights from a new aglaspideid arthropod with caudal appendages from the Furongian of China. *Scientific Reports* 7: 1–18.
- Lewis, P.O. 2001. A likelihood approach to estimating phylogeny from discrete morphological character data. *Systematic Biology* 50: 913–925.
- Lin, H.L. 2008. Early Cambrian (Chiungchussuan, Tsanglangpuan and Lungwangmiaolan). In: Z.Y. Zhou and Y.Y. Zhen (eds.), *Trilobite Record of China*, 36–51. Science Press, Beijing.
- Luo, H.L., Li, Y., Hu, S.X., Fu, X.P., Hou, S.G., Liu, X.Y., Chen, L.Z., Li, F.J., Pang, J.Y., and Liu, Q. 2008. *Early Cambrian Malong Fauna and Guanshan Fauna from Eastern Yunnan, China* [in Chinese, with English summary]. 134 pp. Yunnan Science and Technology Press, Kunming.
- Luo, H.L., Yuan, J.L., Hu, S.X., Yin, J.Y., Zhang, D.Q., and Miao, L.Y. 2015. Ontogeny of the Trilobite *Wutingaspis malungensis* Lu, 1961 [in Chinese, with English abstract]. *Acta Palaeontologica Sinica* 54: 1–11.
- Ortega-Hernández, J., Legg, D.A., and Braddy, S.J. 2013. The phylogeny

- of aglaspidid arthropods and the internal relationships within Artiopoda. *Cladistics* 29: 15–45.
- Ramsköld, L., Chen, J.Y., Edgecombe, G.D., and Zhou, G.Q. 1997. *Cindarella* and the arachnate clade Xandarellida (Arthropoda, early Cambrian) from China. *Earth and Environmental Science Transactions of The Royal Society of Edinburgh* 88: 19–38.
- Ronquist, F., Teslenko, M., van der Mark, P., Ayres, D.L., Darling, A., Höhna, S., Larget, B., Liu, L., Suchard, M.A., and Huelsenbeck, J.P. 2012. MrBayes 3.2: efficient Bayesian phylogenetic inference and model choice across a large model space. *Systematic Biology* 61: 539–542.
- Schmidt, M., Hou, X.G., Zhai, D.Y., Mai, H.J., Belojević, J., Chen, X.H., Melzer, R.R., Ortega-Hernández, J., and Liu, Y. 2022. Before trilobite legs: *Pygmaclypeatus daziensis* reconsidered and the ancestral appendicular organization of Cambrian artiopods. *Philosophical Transactions of the Royal Society B: Biological Sciences* 377: 20210030.
- Scholtz, G. and Edgecombe, G.D. 2006. The evolution of arthropod heads: reconciling morphological, developmental and palaeontological evidence. *Development Genes and Evolution* 216: 395–415.
- Stein, M. 2013. Cephalic and appendage morphology of the Cambrian arthropod *Sidneyia inexpectans*. *Zoologischer Anzeiger* 253: 164–178.
- Størmer, L. 1944. On the relationships and phylogeny of fossil and recent Arachnomorpha: a comparative study on Arachnida, Xiphosura, Eurypterida, Trilobita, and other fossil Arthropoda. *Skrifter Utgitt av det Norske Videnskaps-Akademi i Oslo, Matematisk-Naturvidenskapelig Klasse* 5: 1–158.
- Sun, Z.X., Zeng, H., and Zhao, F.C. 2020. First occurrence of the Cambrian arthropod *Sidneyia* Walcott, 1911 outside of Laurentia. *Geological Magazine* 157: 405–410.
- Walcott, C.D. 1911. Cambrian geology and paleontology II, Middle Cambrian Merostomata. *Smithsonian Miscellaneous Collections* 57: 17–40.
- Zacai, A., Vannier, J., and Lerosee-Aubril, R. 2016. Reconstructing the diet of a 505-million-year-old arthropod: *Sidneyia inexpectans* from the Burgess Shale fauna. *Arthropod Structure and Development* 45: 200–220.
- Zeng, H., Zhao, F.C., Niu, K.C., Zhu, M.Y., and Huang, D.Y. 2020. An early Cambrian euarthropod with radiodont-like raptorial appendages. *Nature* 588: 101–105.
- Zhai, D.Y., Edgecombe, G.D., Bond, A.D., Mai, H.J., Hou, X.G., and Liu, Y. 2019. Fine-scale appendage structure of the Cambrian trilobitomorph *Naraoia spinosa* and its ontogenetic and ecological implications. *Proceedings of the Royal Society B: Biological Sciences* 286: 20192371.
- Zhang, M.Y., Liu, Y., Hou, X.G., Ortega-Hernández, J., Mai, H.J., Schmidt, M., Melzer, R.R., and Guo, J. 2022. Ventral morphology of the non-trilobite artiopod *Retifacies abnormalis* Hou, Chen & Lu, 1989, from the early Cambrian Chengjiang Biota, China. *Biology* 11: 1235.
- Zhang, W.T. and Hou, X.G. 1985. Preliminary notes on the occurrence of the unusual trilobite *Naraoia* in Asia [in Chinese, with English abstract]. *Acta Palaeontologica Sinica* 24: 591–595.
- Zhang, X.L., Fu, D.J., and Dai, T. 2012. A new xandarellid arthropod from the Chengjiang Lagerstätte, Lower Cambrian of southwest China. *Geobios* 45: 335–338.
- Zhao, F.C., Caron, J.-B., Bottjer, D.J., Hu, S.X., Yin, Z.J., and Zhu, M.Y. 2014. Diversity and species abundance patterns of the early Cambrian (Series 2, Stage 3) Chengjiang Biota from China. *Paleobiology* 40: 50–69.
- Zhao, F.C., Hu, S.X., Caron, J.-B., Zhu, M.Y., Yin, Z.J., and Lu, M. 2012. Spatial variation in the diversity and composition of the Lower Cambrian (Series 2, Stage 3) Chengjiang biota, Southwest China. *Palaeogeography, Palaeoclimatology, Palaeoecology* 346: 54–65.
- Zhu, M.Y., Yang, A.H., Yuan, J.L., Li, G.X., Zhang, J.M., Zhao, F.C., Ahn, S.-Y., and Miao, L.Y. 2019. Cambrian integrative stratigraphy and timescale of China. *Science China Earth Sciences* 62: 25–60.